Bound state of an exciton-magnon system under high magnetic fields. I. MnF_2

N. Kojima and M. Kawarazaki
Department of Chemistry, Faculty of Science, Kyoto University, Kyoto 606, Japan

I. Mogi, M. Takeda, G. Kido, and Y. Nakagawa
Institute for Materials Research, Tohoku University, Sendai 980, Japan

(Received 21 September 1992)

We have investigated the bound state of the exciton-magnon transition corresponding to the $^6A_{1g} \rightarrow {}^4A_{1g}, {}^4E_g$ transition in MnF_2 under high magnetic fields. When an external magnetic field was applied along the c axis, this bound state changed dramatically at the spin-flop transition. From the analysis of the field dependence of the bound state, the exciton-magnon interaction responsible for the appearance of the bound state could be elucidated.

I. INTRODUCTION

In magnetic compounds, various types of elementary excitations (excitons, magnons, phonons, etc.) exist. The interaction between these elementary excitations enables them to combine with one another, forming new and more complex excitations such as exciton-magnon transitions (magnon sidebands).

Moreover, this interaction has an effect on the propagation, energy position and shape of the complex excitations. The most dramatic effect is the existence of the bound states below or above the two-particle continuum under certain circumstances.

In the case of the exciton-magnon system, the clear existence of the bound state has been reported only for the magnon sideband in MnF_2.[1,2] However, detailed behavior of this bound state has not yet been reported. Recently, we have observed that a bound state appears on the lowest-energy side of the Cr^{3+} exciton coupled with Yb^{3+} spin flip in $YbCrO_3$ and has a strong dependence on external magnetic field.[3,4]

The subject of the present and the succeeding papers is to investigate the detailed behavior of the bound states of the exciton-magnon system in MnF_2 and $YbCrO_3$ under high magnetic fields and to elucidate the origin of the formation of this bound state. High-field magneto-optics is a powerful method to investigate the propagation of the exciton-magnon system because high fields are able to control the spin structure and the magnetic interaction responsible for the migration of magnetic elementary excitations.

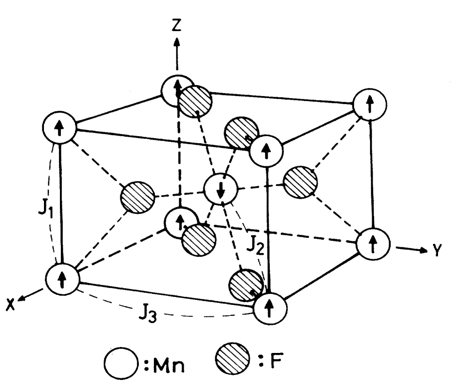

FIG. 1. The crystal and spin structures of MnF_2. Exchange parameters for various pairs of ions are indicated in the figure.

We briefly summarize important properties of MnF_2. The crystal has a rutile-type structure belonging to the space group $P4_2/mnm$ with lattice constants of $a = 4.8734$ Å and $c = 3.3099$ Å at room temperature.[5] Below $T_N (= 67.336$ K),[6] the spins of Mn^{2+} order antiferromagnetically along the c axis, the body-center ions of the unit cell forming the down-spin sublattice, and the corner ions the up-spin sublattice,[7] which is shown in Fig. 1. When an external magnetic field is applied along the c axis at 4.2 K, the spin-flop transition takes place at 9.3 T.[8] The exchange parameters J_1, J_2, and J_3 shown in Fig. 1 were estimated to be -0.22,[9] 1.22,[10] and -0.035 cm^{-1},[9] respectively.

II. EXPERIMENTAL PROCEDURE

The single crystals of MnF_2 used in the measurements were produced by Furuuchi-kagaku Co., Tokyo. The directions of the crystal axis were determined by the Laue method.

Magnetic fields up to 6 T were produced by a Helmholtz-type superconducting magnet, and steady magnetic fields up to 23 T were generated by a hybrid magnet at Tohoku University.

For the spectroscopic measurement under the magnetic field up to 6 T, a Jobin Yvon THR1500 spectrometer was used with an HTV-R376 photomultiplier. Photoelectric signals were amplified and converted into logarithmic scale and recorded. For the spectroscopic measurement under the magnetic field up to 23 T, a Jobin Yvon THR1000 spectrometer with an optical fiber system was used.

III. EXPERIMENTAL RESULT

Figure 2 shows the optical absorption spectra corresponding to the $^6A_{1g} \rightarrow {}^4A_{1g}$, ^4E_g transition in MnF_2 at 4.2 K. Meltzer, Chen, and Lowe-Pariseau observed these spectra and found a large negative dispersion of the $M_{2\pi}$

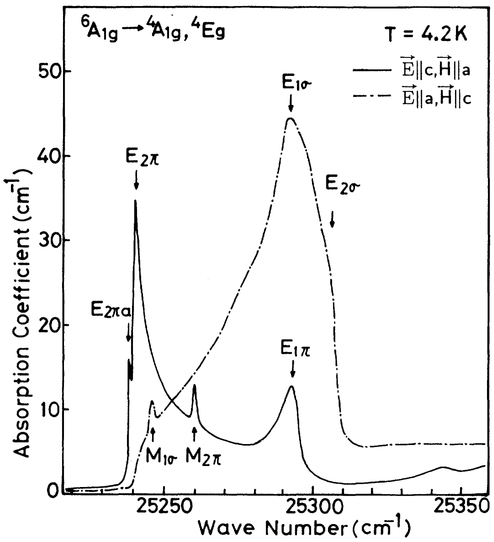

FIG. 2. Optical absorption spectra in the lowest-energy region of the $^6A_{1g} \rightarrow {}^4A_{1g}, {}^4E_g$ transition of Mn^{2+} in MnF_2 at 4.2 K. **E** and **H** denote the electric and magnetic vectors of the incident light.

exciton and a bound state of the magnon sideband accompanied by the $M_{2\pi}$ exciton.[1] The sharp absorption lines $M_{1\sigma}$ and $M_{2\pi}$ are magnetic dipole lines and are assigned to the exciton states of the $^6A_{1g} \rightarrow {}^4E_g$ transition. $E_{1\sigma,\pi}$ and $E_{2\sigma,\pi}$ are the magnon sidebands of the $M_{1\sigma}$ and $M_{2\pi}$ excitons, respectively.

According to Meltzer *et al.*,[1,2] for the E_u component of the ^4E_g state in MnF_2, the exchange interaction responsible for the exciton transfer along the c axis is extraordinarily large because the nearest neighbors along the c axis have the same spin orientations and the exciton transfer is spin allowed. As a result, the $M_{2\pi}$ exciton of the ^4E_g state in MnF_2 has a large negative dispersion, which is reflected in the sharp cutoff profile at the lowest-energy side of the $E_{2\pi}$ magnon sideband. Using the following exciton dispersion,

$$E_k = 2K_1 \cos(ck_z) + 2K_3\{\cos(ak_x) + \cos(ak_y)\} , \quad (1)$$

where K_1 and K_3 are the exciton transfer coefficients for the first- and third-neighbor ions, the exciton dispersions for $M_{1\sigma}$ and $M_{2\pi}$ have been estimated to be ($2K_1 = 2$ cm^{-1}, $2K_3 = 1$ cm^{-1}) and ($2K_1 = 37$ cm^{-1}, $2K_3 = 0$ cm^{-1}), respectively.[2]

A Sharp line which appeared at the lower-energy side of the $E_{2\pi}$ magnon sideband has been identified as a exciton-magnon bound state.[1,2] The exciton-magnon bound state in MnF_2 has been suggested to be a Davydov split component induced by the resonance effect of exciton-magnon pair between the nearest two sublattices.[11] We have investigated the behavior of this bound state under high magnetic fields in order to make clear the formation mechanism.

Figure 3 shows the behavior of the lower-energy side of the magnon sideband of the $^6A_{1g} \rightarrow {}^4E_g$ transition in MnF_2 under magnetic fields. In the case of $\mathbf{H}_0 \| \mathbf{a}$, there is no appreciable spectral change in magnetic fields up to 6 T. On the other hand, in the case of $\mathbf{H}_0 \| \mathbf{c}$, when an external magnetic field is applied up to 5.7 T, the bound state $E_{2\pi a}$ of the $E_{2\pi}$ magnon sideband splits into two lines. The $M_{2\pi}$ line, which is the original exciton of the $E_{2\pi}$ magnon sideband, also splits into two lines. Figure 4 shows the field dependence of the energy positions of the $E_{2\pi a}$, $E_{2\pi}$, and $M_{2\pi}$ peaks. When an external magnetic field is applied along the c axis of MnF_2, the effective field on the Mn^{2+} sublattice with $S_z = S$ is different from that with $S_z = -S$, which causes the sublattice splitting. The sublattice splittings of the exciton line and its magnon

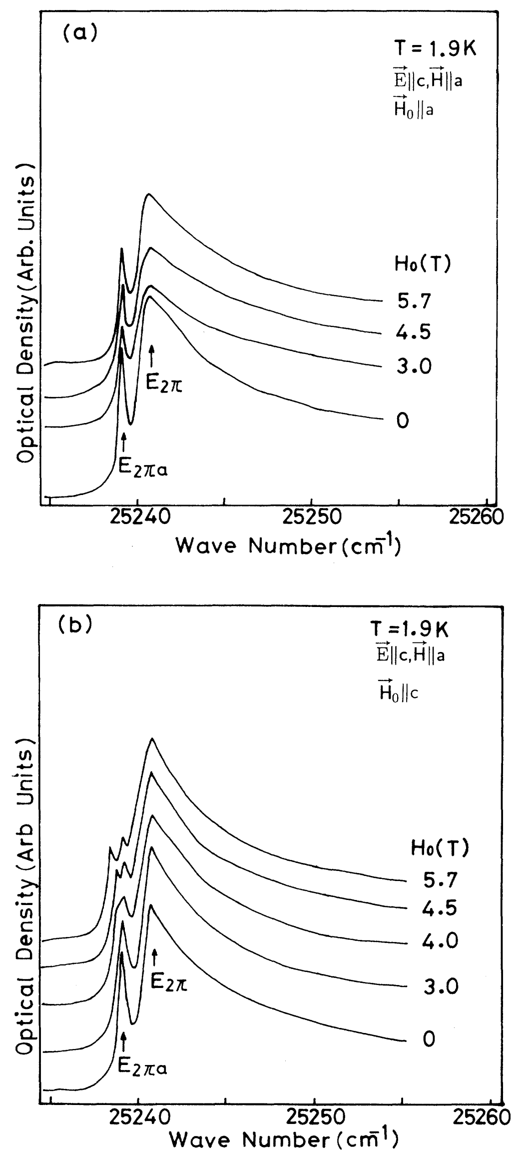

FIG. 3. Behavior of the lowest-energy region of the $E_{2\pi}$ magnon sideband and its bound state $E_{2\pi a}$ in MnF_2 in the magnetic fields H_0 parallel and perpendicular to the c axis. (a) $\mathbf{H}_0 \| \mathbf{a}$. (b) $\mathbf{H}_0 \| \mathbf{c}$.

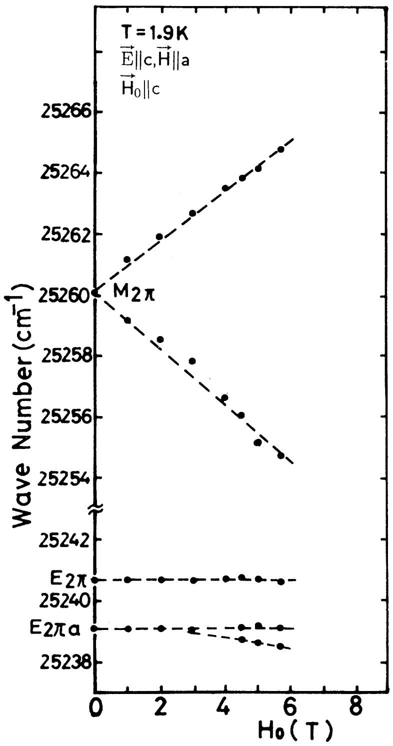

FIG. 4. Magnetic field dependence of the energy positions of the $M_{2\pi}$, $E_{2\pi}$, and $E_{2\pi a}$ peaks. The magnetic field $\mathbf{H}_0 \| \mathbf{c}$.

sideband corresponding to the ${}^6A_{1g} \rightarrow {}^4E_g$ transition are described as

$$\Delta E^{\mathrm{ex}} = |5g_c - 3g_c^*|\mu_B H_0 \tag{2}$$

and

$$\Delta E^{\mathrm{ex+mag}} = |3g_c - 3g_c^*|\mu_B H_0 \ , \tag{3}$$

respectively, where g_c and g_c^* are the g values of the ground and the excited states, respectively. Using Eqs. (1) and (2), $g_c = 2.0$, $\Delta E^{\mathrm{ex}}(M_{2\pi})/2\mu_B H_0 = 2.2$, $\Delta E^{\mathrm{ex+mag}}(E_{2\pi})/2\mu_B H_0$ is estimated to be 0.19, which is almost identical with the experimental value $\Delta E(E_{2\pi a})/2\mu_B H_0 = 0.18$. Therefore, the splitting of the bound state $E_{2\pi a}$ with $\mathbf{H}_0 \| \mathbf{c}$ is concluded to be the sublattice splitting.

As shown in Fig. 4, the center of the $M_{2\pi}$ exciton remains unchanged under the magnetic field up to 6 T. On the contrary, the center of the bound state $E_{2\pi a}$ shifts to the lower-energy side with increasing magnetic field. That is, the binding energy of the exciton-magnon bound state increases with increasing magnetic field along the c axis.

Figure 5 shows the behavior of the magnon sideband and its bound state under high magnetic fields parallel to the c axis. Figure 6 shows the lower-energy side of the $E_{2\pi}$ magnon sideband. When an external magnetic field is applied along the c axis, the spin-flop transition takes place at H_{SF} (9.3 T). As shown in Figs. 5 and 6, the magnon sideband remains almost unchanged at H_{SF}. On the contrary, the bound state $E_{2\pi a}$ changes dramatically in its intensity and energy position at H_{SF}. The profile of the bound state in the spin-flop phase is very different from that of the bound state in the antiferromagnetic phase, and it resembles closely the band shape of the lowest-energy region of the $E_{2\pi}$ magnon sideband. Strange to say, the bound state and the lowest-energy side of the $E_{2\pi}$ magnon sideband consist of two peaks in the spin-flop phase, in spite that the sublattice splitting of the magnon sideband vanishes above H_{SF}.

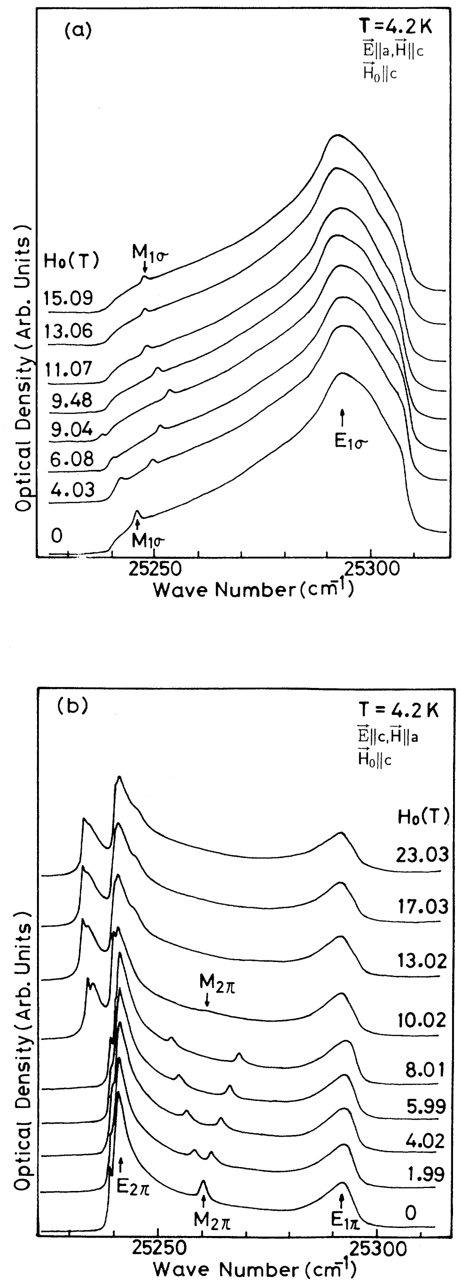

FIG. 5. Behavior of the magnon sidebands of the $M_{1\sigma}$ and $M_{2\pi}$ excitons in MnF_2 in the magnetic field parallel to the c axis. (a) $\mathbf{E}\|\mathbf{a}$, $\mathbf{H}\|\mathbf{c}$. (b) $\mathbf{E}\|\mathbf{c}$, $\mathbf{H}\|\mathbf{a}$.

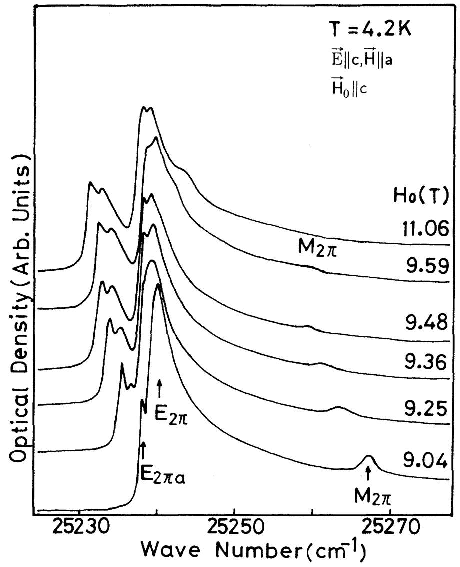

FIG. 6. Behavior of the lowest-energy region of the $E_{2\pi}$ magnon sideband and its bound state $E_{2\pi a}$ in MnF_2 in the magnetic fields around H_{SF} (9.3 T). The magnetic field $\mathbf{H}_0 \| \mathbf{c}$.

IV. DISCUSSION

In this section, we discuss the detailed behavior of the exciton-magnon bound state in MnF_2 under high magnetic fields and elucidate the origin of this bound state. In the energy region of the ${}^6A_{1g} \rightarrow {}^4A_{1g}, {}^4E_g$ transition in MnF_2, a very sharp line $E_{2\pi a}$ typical of a bound state appears on the lower-energy side of the $E_{2\pi}$ magnon sideband.[1,2] The origin of this bound state has been theoretically investigated by several authors.[11–13] In connection with this problem, Tanabe and Aoyagi has suggested the following concept.[13] If an exciton and a magnon are created on A and B sublattices, respectively, outside the range of nearest-neighbor exchange interaction J, their energy will be $E^{ex}+E^{mag}$. To excite an exciton and a magnon on nearest-neighbor sites will cost an amount of energy $E^{ex}+E^{mag}-2JS\{(J'S'/JS)-1\}\pm L$, where J' is the exchange integral between the excited and ground states and $S'=S-1$. $L=2K(ij)/(2S-1)$ is the resonance effect of the exciton-magnon pair between the nearest two sublattices, which is schematically shown in Fig. 7. According to Tanabe and Aoyagi,[13] the resonance term $\pm L$ is responsible for the appearance of the bound state $E_{2\pi a}$ of the $E_{2\pi}$ magnon sideband in MnF_2 and the energy difference between $E_{2\pi a}$ and $E_{2\pi}$ is $-2JS\{(J'S'/JS)-1\}-L$. If this concept is true, the bound state $E_{2\pi a}$ does not undergo a sublattice splitting under external magnetic fields because the bound state is already split by the resonance term $\pm L$ at zero field.

As shown in Fig. 3(b), however, the exciton-magnon bound state $E_{2\pi a}$ shows the sublattice splitting under the magnetic field parallel to the c axis, which implies that the resonance effect $\pm L$ is negligibly small and is not responsible for the appearance of the exciton-magnon bound state.

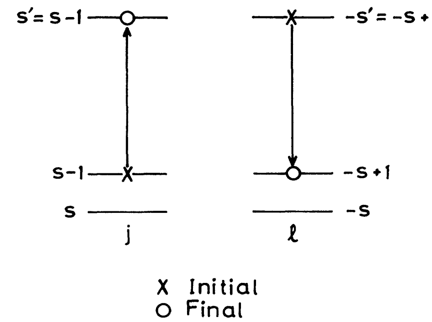

FIG. 7. Resonance effect of an exciton-magnon pair between the nearest two sublattices (Ref. 13).

Now, we consider another exciton-magnon interaction responsible for the origin of the bound state. As mentioned in Sec. III, the negative dispersion of the $M_{2\pi}$ exciton is one dimensional and large enough to push the magnon sideband $E_{2\pi}$ to the lower-energy side of the $M_{2\pi}$ exciton line. Therefore, $E_{2\pi}$ is the exciton-magnon state at the Brillouin zone edge, where the exciton-magnon interaction acts most effectively. Moreover, it should be noted that the $M_{2\pi}$ exciton is one dimensional and a one-dimensional system is most strongly localized by the deformed potential.[14] Thus, we arrived at the following concept. The exciton-magnon interaction $-2JS\{(J'S'/JS)-1\}$ shifts the exciton-magnon states at the Brillouin zone edge towards the lower-energy side, whose deformed energy is probably responsible for the appearance of the bound state.

Next, we discuss the magnon sideband in the spin-flop phase. The continuous spectrum of the magnon sideband remains almost unchanged at the spin-flop transition H_{SF}. At H_{SF}, the energy shifts of the $M_{1\sigma}$ and $M_{2\pi}$ excitons are $+2.0$ and ~ 0 cm^{-1}, respectively, and the energy shift of the zone-boundary magnon is about -2 cm^{-1}.[15] Thus, it is reasonable that the energy shifts of the magnon sidebands $E_{1\sigma}$ and $E_{2\pi}$ at H_{SF} are very small.

On the contrary, the bound state $E_{2\pi a}$ changes dramatically in its intensity and energy position at H_{SF}, which implies that the exciton-magnon interaction responsible for the formation of the exciton-magnon bound state changes discontinuously at H_{SF}. In the spin-flop phase, the profile of the bound state $E_{2\pi a}$ resembles closely that of the lowest-energy region $E_{2\pi}$ of the magnon sideband. Both $E_{2\pi a}$ and $E_{2\pi}$ consist of two peaks in spite of the fact that the sublattice splitting of the magnon sideband vanishes above H_{SF}.

From these results, one arrives at the following conclusion. At the spin-flop transition, the resonance effect $\pm L$ of exciton-magnon pair between the nearest two sublattices becomes large, which splits the magnon sideband $E_{2\pi}$ at the Brillouin zone boundary into two branches. Consequently, two similar branches appear on the lower-energy region of the magnon sideband. A sharp line typical of a bound state appears on the lowest-energy side of each branch of the magnon sideband, which is caused by the exciton-magnon interaction $-2JS\{(J'S'/JS)-1\}$.

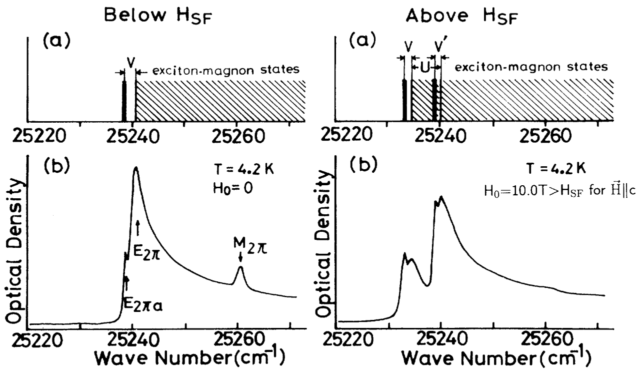

FIG. 8. $E_{2\pi}$ magnon sideband and its bound state in MnF_2 below and above the spin-flop transition H_{SF} (9.3 T). (a) Scheme of the energy spectrum. (b) Absorption spectrum. $U=2L$, V (or V')$=|2JS\{(J'S'/JS)-1\}|$.

V. CONCLUSION

In the energy region of the ${}^6A_{1g}\rightarrow{}^4A_{1g},{}^4E_g$ transition in MnF_2, a bound state appears on the lowest-energy side of the magnon sideband $E_{2\pi}$. We have investigated the detailed behavior of this exciton-magnon bound state in MnF_2 by means of high-field magneto-optics, which is summarized as follows.

(i) $0<H_0<H_{SF}(=9.3$ T). When an external magnetic field is applied along the spin easy axis ($H_0\|\mathbf{c}$), the bound state $E_{2\pi a}$ of the $E_{2\pi}$ magnon sideband takes place on the sublattice splitting. Therefore, the origin of the appearance of the exciton-magnon bound state is not the resonance effect $\pm L$ of the exciton-magnon pair between the nearest two sublattices, but the exciton-magnon interaction $-2JS\{(J'S'/JS)-1\}$. In the antiferromagnetic phase, the binding energy of the exciton-magnon bound state increases with increasing magnetic field along the c axis.

(ii) $H_0>H_{SF}(=9.3$ T). The bound state $E_{2\pi a}$ changes dramatically at the spin-flop transition H_{SF}. In the spin-flop phase, the resonance effect $\pm L$ of the exciton-magnon pair becomes large, which splits the magnon sideband at the Brillouin zone edge into two components. Consequently, two similar branches appear on the lower-energy side of the magnon sideband. Moreover, a sharp line typical of a bound state appears on the lowest-energy side of each branch of the magnon sideband, which is induced by the exciton-magnon interaction $-2JS\{(J'S'/JS)-1\}$. This conclusion is schematically shown in Fig. 8, and the estimated values of the exciton-magnon interactions in the antiferromagnetic and the spin-flop phases are listed in Table I.

TABLE I. Exciton-magnon interaction for the $E_{2\pi}$ magnon sideband in MnF_2 at 4.2 K.

H_0	$U=2L$ (cm^{-1})	$V=\|2JS\{(J'S'/JS)-1\}\|$ (cm^{-1})
Below H_{SF} ($H_0=0$)	0	1.6
Above H_{SF} ($H_0=10.0T$)	5.5	1.4, 1.2

[1]R. S. Meltzer, M. Y. Chen, M. Lowe-Pariseau, and D. S. McClure, Phys. Rev. Lett. **21**, 913 (1968).
[2]R. S. Meltzer, M. Lowe, and D. S. McClure, Phys. Rev. **180**, 561 (1968).
[3]N. Kojima and I. Tsujikawa, J. Phys. (Paris) Colloq **49**, C8-1461 (1988).
[4]N. Kojima (unpublished).
[5]M. Griffel and J. W. Stout, J. Am. Chem. Soc. **72**, 4351 (1950).
[6]P. Heller and G. B. Benedek, Phys. Rev. Lett. **8**, 428 (1962).
[7]R. A. Erickson, Phys. Rev. **90**, 779 (1953).
[8]I. S. Jacobs, J. Appl. Phys. **32**, 1289 (1962).
[9]A. Okazaki, K. C. Tuberfield, and R. W. H. Stevenson, Phys. Lett. **8**, 9 (1964).
[10]C. Trapp and J. W. Stout, Phys. Rev. Lett. **10**, 157 (1963).
[11]S. Freeman and J. J. Hopfield, Phys. Rev. Lett. **21**, 910 (1968).
[12]T. Fujiwara and Y. Tanabe, J. Phys. Soc. Jpn. **39**, 7 (1975).
[13]Y. Tanabe and K. Aoyagi, in *Excitons,* edited by E. I. Rashba and M. D. Sturge (North-Holland, Amsterdam, 1982), p. 603.
[14]V. L. Berezinskii, Zh. Eksp. Teor. Fiz. **65**, 1251 (1973) [Sov. Phys. JETP, **38**, 620 (1974)].
[15]T. Bernstein, A. Misetich, and B. Lax, Phys. Rev. B **6**, 979 (1972).